XVII European Conference
ECSMGE 2019
Reykjavík
on Soil Mechanics
and Geotechnical Engineering

Acoustic emission monitoring in geotechnical element tests

Surveillance des émissions acoustiques dans les essais d'éléments géotechniques

A. Smith, T. Biller, H. J. Heather-Smith, N. Dixon and J. A. Flint
Loughborough University, Leicestershire, UK

ABSTRACT: Acoustic emission (AE) is high-frequency noise (>10kHz) generated by deforming materials. AE is widely used in many industries for non-destructive testing and evaluation; however, it is seldom used in geotechnical engineering, despite evidence of the benefits, because AE generated by particulate materials is highly complex and difficult to measure and interpret. This paper demonstrates that innovative AE instrumentation and measurement can enhance insights into geotechnical element tests. Results from a programme of triaxial compression and shear, large direct-shear and large permeameter experiments show that AE can be used to characterise mechanical and hydromechanical behaviour of soils and soil-structure interaction, including: dilative shear behaviour; transitions from pre- to post-peak shear strength; changes in strain rates; isotropic compression; unload-reload cycles of compression and shear; and seepage-induced internal instability phenomena.

RÉSUMÉ: L'émission acoustique (AE) est un bruit haute fréquence (> 10 kHz) généré par des matériaux déformants. L'AE est largement utilisé dans de nombreux secteurs pour les tests et l'évaluation non destructifs; Cependant, il est rarement utilisé en génie géotechnique, malgré les avantages évidents, car les effets indésirables générés par les particules sont extrêmement complexes et difficiles à mesurer et à interpréter. Cet article démontre qu'une instrumentation et une mesure AE innovantes peuvent améliorer la compréhension des tests d'éléments géotechniques. Les résultats d'un programme d'expériences sur la compression et le cisaillement triaxiaux, le grand cisaillement direct et le grand perméamètre montrent que l'EA peut être utilisé pour caractériser le comportement mécanique et hydromécanique des sols et leurs interactions structure-sol, notamment: le comportement de cisaillement dilatif; les transitions de résistance au cisaillement avant et après le pic; les changements de taux de déformation; compression isotrope; cycles déchargement-rechargement de la compression et du cisaillement; et les phénomènes d'instabilité interne induits par les infiltrations.

Keywords: Acoustic Emission; Deformation; Instrumentation; Laboratory tests; Monitoring

1 INTRODUCTION

Proportions of the energy dissipated during deformation of, and seepage through, particulate materials are converted to heat and sound. The high-frequency (>10kHz) component of this sound energy is called acoustic emission (AE).

AE monitoring offers the potential to sense particle-scale behaviours that lead to macro-scale responses of granular materials (Smith & Dixon, 2019). AE is widely used in many industries for non-destructive testing and evaluation of materials and systems (e.g. pipe networks and

pressure vessels); however, it is seldom used in geotechnical engineering, despite evidence of the benefits, because AE generated by particulate materials is highly complex and difficult to measure and interpret.

AE is generated by deformation of soil bodies and soil-structure systems through a suite of mechanisms, including: inter-particle friction; particle contact network rearrangement (e.g. release of contact stresses and stress redistribution); degradation of particle asperities; particle crushing; and friction at the interface between the soil and structural element (Michlmayr & Or, 2014; Smith et al. 2017; Heather-Smith et al. 2018; Smith & Dixon, 2019). AE is also generated by seepage-induced internal erosion mechanisms through: frictional interactions between particles; friction due to fluid flow through the soil; collisions of migrating particles; and collapse of structure (e.g. suffosion) (Biller et al. 2018).

Fundamental laboratory studies on the AE behavior of soils were carried out in the 1970s, 1980s and 1990s (e.g. Koerner et al. 1981; Tanimoto & Tanaka 1986). Recent advances have been made in the interpretation of soil-structure interaction behavior from AE measurements using physical modelling and field experiments for slope instability (Smith et al. 2014; Smith & Dixon 2015; Smith et al. 2017; Berg et al. 2018; Dixon et al. 2018) and buried pipe deformation applications.

This paper demonstrates how innovative AE instrumentation and measurement can enhance insights into geotechnical element tests using examples from triaxial compression and shear, large direct-shear and large permeameter experiments.

2 AE MEASUREMENT

The fundamental components of an AE measurement system are shown in Figure 1. The AE sensor converts the mechanical waves to a voltage waveform, which is then amplified and filtered to improve the signal-to-noise ratio.

Analogue-to-digital conversion samples the waveform to produce a data series. Signal analysis and data storage are typically performed on a laptop or PC based system.
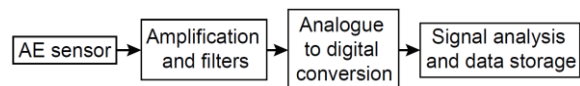

Figure 1. AE measurement system components

AE signal analysis can be performed using many different parameters and algorithms in both time and frequency domains (e.g. rise time, peak amplitude, dominant frequency). The research reported here measured ring-down count (RDC) rates, which are the number of times the AE waveform crosses a programmable threshold within a predefined time interval and are a measure of the signal energy. The Authors have also measured *b-values* in previous studies (e.g. Smith & Dixon, 2019), which correlate strongly with physical behaviours; however, space precludes the inclusion of additional *b-value* time series here.

A body of research has demonstrated that deforming soils generate significant AE within the frequency range of 10-100 kHz (e.g. Koerner et al. 1981; Smith & Dixon, 2019). Filtering signals below 10 kHz is essential to remove extraneous low-frequency environmental noise that could be generated in a laboratory or field environment. Mao & Tohata (2015) demonstrated that AE generated by particle crushing has significant energy above 100 kHz. The research reported here filtered signals above 100 kHz as relatively low confining stresses were investigated ($\leq$ 300 kPa) and particle damage was minimal (confirmed from post-test particle size distributions).

The AE sensor used was a MISTRAS R3α piezoelectric transducer, which is sensitive over the frequency range of 0-100 kHz and has a resonant frequency of 30 kHz. The AE measurement system was a bespoke setup comprising a pre-amplifier (with a 10-1200 kHz filter and 20 dB gain) a main amplifier (with a 10-

100 kHz filter and 3 dB gain), an analogue-to-digital converter with 2 M samples/second sampling frequency, and a laptop computer with a LabView program to condition, process and record the AE waveform. This measurement system applied a total gain of 23 dB and constrained the response to within 10-100 kHz.

3 TRIAXIAL TESTING

A hydraulic GDS Bishop and Wesley stress path triaxial apparatus was used to eliminate noise that could be generated by motor-operated systems. Figure 2 shows the bespoke 50 mm diameter base pedestal developed to incorporate both AE and pore-water pressure measurement.
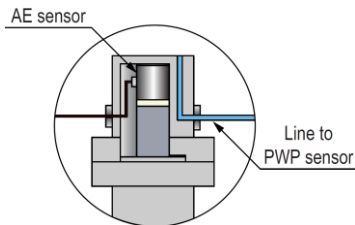

Figure 2. Bespoke base pedestal

Sand specimen preparation followed a similar procedure to that described in Been et al. (1991). The cylindrical specimens were 50 mm in diameter and 100 mm tall. Samples were prepared in a membrane-lined split-mould mounted on the base pedestal. Moist compacted samples were tamped into the mould to a target relative density, D_r, in 10 equal layers. Back pressure saturation (Been et al. 1991) of 400 kPa was imposed under a constant effective stress of approximately 20 kPa until a minimum Skempton's B parameter of 0.97 was measured. Isotropic compression was performed by increasing the cell pressure to achieve a target effective stress (e.g. 100, 200 or 300 kPa). Drained shearing was performed strain-controlled through application of a constant rate of axial displacement. A summary of the triaxial tests described in this paper is shown in Table 1. The particle size distributions of the Leighton Buzzard sand (LBS) are shown in Figure 3.

Table 1. Summary of the drained triaxial isotropic compression and shearing tests

Test No.	Material	σ'_r[+]	Axial velocity (mm/hr)	D_r[x]
1	LBS 8/16	100	1	84
2	LBS 8/16	200	1	84
3	LBS 8/16	300	1	84
4	LBS Combined	300	1, 3, 6	82
5[$]	LBS 8/16	300	6	84

[+] Final effective confining pressure (kPa) after isotropic compression and constant during shearing.
[x] Initial relative density (%) prior to isotropic compression.
[$] Isotropic load-unload-reload (LUR) cycles of cell pressure followed by LUR cycles of deviator stress.
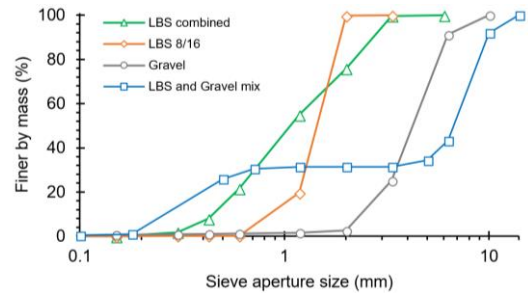Note: All specimens failed with a concentrated shear zone in shearing.

Figure 3. Particle size distributions for materials used in presented studies

Figure 4 shows AE versus shear strain from triaxial Tests 1, 2 and 3 to demonstrate the influence of stress level. An increase in effective confining pressure caused a proportional increase in AE rates during shearing, and a greater range of shear strain before constant AE rates were reached (i.e. consistent with the volumetric strain behaviour whereby contraction was extended over a greater range of shear strain).
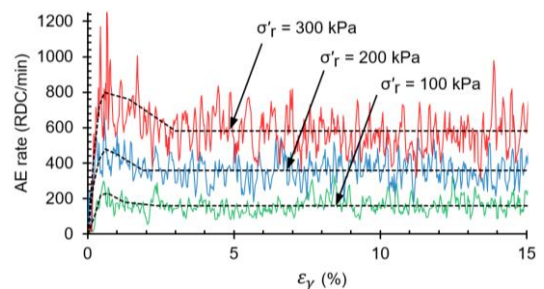

Figure 4. AE rate versus shear strain from triaxial Tests 1, 2 and 3

Stepped increases in axial displacement rate were imposed during Test 4 (Figure 5) when post-peak conditions were established to investigate the AE response to accelerating deformation behaviour. The average post-peak AE rates for 6 mm/hr and 3 mm/hr were 6.2 and 2.8 times greater than those generated at 1 mm/hr, respectively, demonstrating that measured AE rates are proportional to the rate of shear strain. Smith & Dixon (2019) present quantified relationships between AE, stress level and shear strain rate. In addition, Smith & Dixon (2019) present a framework to interpret the transition from contractive to dilative behaviour and mobilisation of peak shear strength in dense sands using AE measurements.

Figure 6 (Test 5) demonstrates that the Kaiser Effect occurs in particulate materials under cycles of both isotropic compression and deviator stress: AE activity is negligible until the current stress conditions (compression and/or shear) exceed the maximum that the soil has been subjected to in the past.

4   DIRECT-SHEAR TESTING

Tests of interface shear between soil and steel are being performed using large direct-shear apparatus (Wille Geotechnik, ADS-300) to develop an approach to interpret soil-structure interaction-generated AE (Figure 7).

Figure 8 shows measurements from a direct-shear test performed with dense (initial D_r of 80%), subangular-subrounded gravel (8-12 mm, Figure 3) shearing against a steel plate. A normal stress of 150 kPa and a constant shearing rate of 2 mm/min was applied.

Shearing resistance was rapidly mobilised and then remained relatively constant after approximately 2.5 mm of shear displacement. This shear stress versus shear displacement behaviour is characteristic of interface shear between steel and granular media (e.g. Ho et al. 2011).
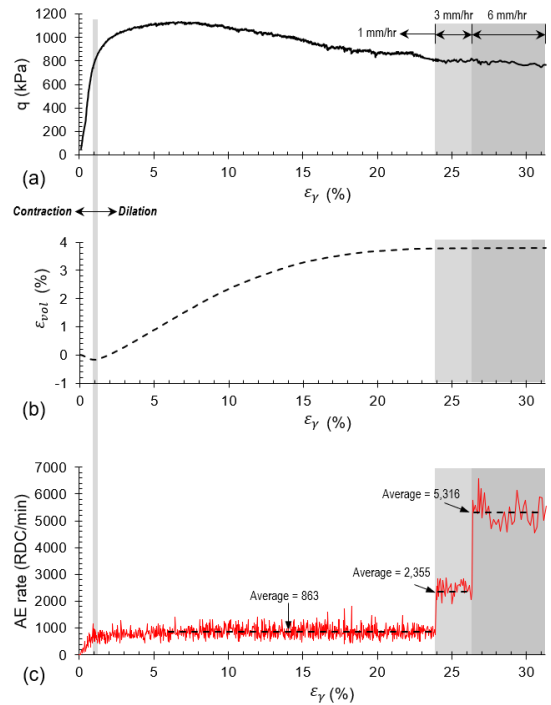

Figure 5. Measurements versus shear strain from Test 4: (a) deviator stress; (b) volumetric strain (dilation shown as positive); and (c) AE rate
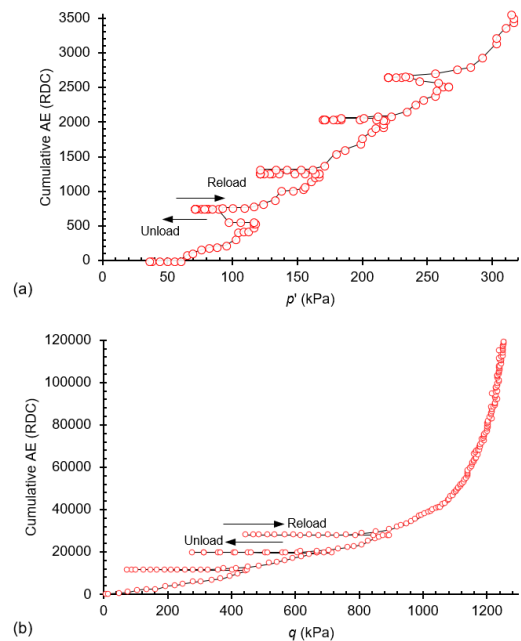

Figure 6. Measurements from load-unload-reload cycles (Test 5) of mean effective stress in isotropic compression (a) and deviator stress in shearing (b)
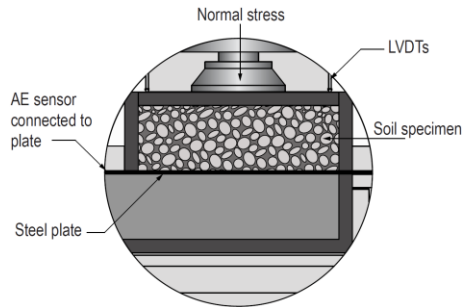
Figure 7. Schematic cross-section of the large direct-shear apparatus
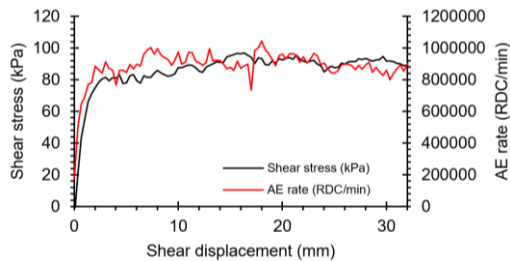

Figure 8. Shear stress and AE rate versus shear displacement

The AE rate measurements followed this same trend in behaviour, increasing linearly proportionally with shear stress during mobilisation of shearing resistance, and then remaining relatively constant thereafter. These results show that AE can be used to measure pre- and post-peak shear strength behaviour, which is critical for health monitoring: accelerating deformation behaviour typically ensues following mobilisation of peak shear strength and this ultimate limit state can have devastating consequences for people and infrastructure.

5 PERMEAMETER TESTING

Seepage-induced internal erosion experiments are being performed using large permeameter apparatus to investigate the AE generated from internally unstable soils subjected to a range of hydraulic regimes. A cross-section of the current permeameter apparatus is shown in Figure 9. A new permeameter is being developed to enable application of vertical effective stresses. A suite of hydrophones in addition to piezoelectric

transducers will be installed for AE measurement in the new apparatus. The existing apparatus employs a waveguide, installed perpendicular to the direction of flow, to transmit AE to the sensor.
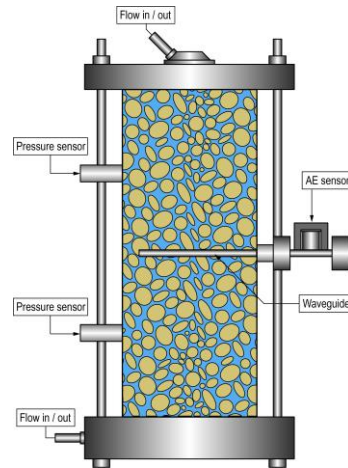

Figure 9. Schematic cross-section of the large permeameter apparatus (specimen of 160 mm diameter and 400 mm tall)

Figure 10 shows time series measurements of hydraulic gradient and AE rate from a test performed on a LBS and Gravel mix (Figure 3). The LBS and Gravel mix is classed as internally unstable under all geometric criteria (e.g. Chang & Zhang, 2013). The soil was pluviated under a head of water to form the specimen. The permeameter was oriented horizontally with a constant head applied of approximately 1.1 m.
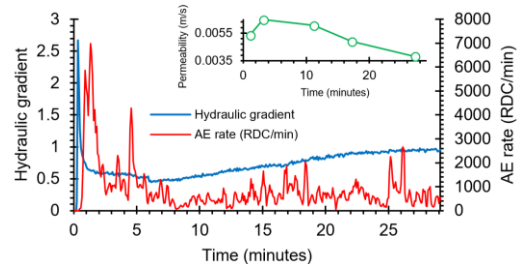

Figure 10. Hydraulic gradient and AE rate vs time

AE generation began rapidly at the onset of head application, and varied with the measured hydraulic gradient, which controlled the soil internal stability conditions. The specimen was under self weight only, with no additional normal

stress applied, and hence fluidisation (i.e. the particles were forced apart, volumetric increase) in addition to the migration of particles (observed during the experiment) caused AE generation.

6 SUMMARY AND FUTURE WORK

This paper has demonstrated how innovative AE instrumentation and measurement can enhance insights into geotechnical element tests. Results from triaxial, direct-shear and permeameter experiments were presented to show that AE generation is related to soil and soil-structure interaction behaviour, including: dilative shear behaviour; transitions from pre- to post-peak shear strength; changes in strain rates; isotropic compression; unload-reload cycles of compression and shear; and seepage-induced internal instability phenomena.

A programme of research is ongoing to establish quantitative interpretation of AE generated by soil bodies and soil-structure systems. This new knowledge will enable use of AE monitoring for early warning of serviceability and ultimate limit state failures in the field.

7 ACKNOWLEDGEMENTS

8 REFERENCES

Been, K., Jefferies, M.G. & Hachey, J. 1991. Critical state of sands. *Géotechnique*, 41(3), 365-381.

Berg, N., Smith, A., Russell, S., Dixon, N., Proudfoot, D. & Take, W.A. 2018. Correlation of acoustic emissions with patterns of movement in an extremely slow moving landslide at Peace River, Alberta, Canada. *Canadian Geotechnical Journal* 55(10): 1475-1488.

Biller, T., Smith, A. & Dixon, N. 2018. Early detection of seepage-induced internal erosion using acoustic emission monitoring. *15th BGA YGES*, *University of Surrey*, UK, 2-3 July.

Chang, D.S. & Zhang, L.M. 2013. Extended internal stability criteria for soils under seepage. *Soils and Foundations*, 53(4), 569-583.

Dixon, N., Smith, A., Flint, J.A., Khanna, R., Clark, B. & Andjelkovic, M. 2018. An acoustic emission landslide early warning system for communities in low-income and middle-income countries. *Landslides*, 15(8), 1631–1644.

Heather-Smith, H.J., Smith. A., Dixon. N., Flint. J.A. & Wordingham. J. 2018. Monitoring buried infrastructure deformation using acoustic emissions. *9th European Workshop on Structural Health Monitoring*, July 10-13, Manchester, UK.

Ho, T.Y.K., Jardine, R.J. & Anh-Minh, N. 2011. Large-displacement interface shear between steel and granular media. *Géotechnique*, 61(3), 221-234.

Koerner, R.M., McCabe, W.M. & Lord, A.E. 1981. Acoustic emission behavior and monitoring of soils. In *Acoustic emissions in geotechnical engineering practice* (eds V. P. Drnevich and R. E. Gray), ASTM STP 750, pp. 93–141. West Conshohocken, PA, USA: ASTM International.

Mao, W. & Towhata, I. 2015. Monitoring of single-particle fragmentation process under static loading using acoustic emission. *Applied Acoustics*, 94, 39-45.

Michlmayr, G. & Or, D. 2014. Mechanisms for acoustic emissions generation during granular shearing. *Granular Matter*, 16(5), 627-640.

Smith, A. & Dixon, N. 2015. Quantification of landslide velocity from active waveguide–generated acoustic emission. *Canadian Geotechnical Journal*, 52(4), 413-425.

Smith, A. & Dixon, N. 2019. Acoustic emission behaviour of dense sands. *Géotechnique*. (10.1680/jgeot.18.P.209).

Smith, A., Dixon, N., Meldrum, P., Haslam, E. & Chambers, J. 2014. Acoustic emission monitoring of a soil slope: Comparisons with continuous deformation measurements. *Géotechnique Letters*, 4(4), 255-261.

Smith, A., Dixon, N. & Fowmes, G. 2017. Early detection of first-time slope failures using acoustic emission measurements: large-scale physical modelling. *Géotechnique*, 67(2), 138-152.

Tanimoto, K. & Tanaka, Y. 1986. Yielding of soil as determined by acoustic emission. *Soils and foundations*, 26(3), 69-80.